

دراسة تأثير العيوب على الكفاءة الكمية لخلايا البيروفسكايت الشمسية

هاجر خليل ابراهيم احمد محمد السبعواي قيس ذنون الجواري
كلية هندسة الالكترونيات / جامعة نينوى / قسم الالكترونيات

(قدم للنشر ٢٠٢١/٨/١٩ قبل للنشر ٢٠٢١/٩/١٢)

الملخص

اكتسبت خلايا البيروفسكايت الشمسية (PSCs) اهتمامًا كبيرًا بمجال الطاقة الشمسية في ظل التطور السريع لتكنولوجيا التصنيع ، مما جعل خلايا بيروفسكايت الشمسية عالية الكفاءة والصدقية للبيئة أكثر جاذبية كمرشح بديل لتوليد الطاقة. تؤثر العيوب في الطبقة الماصة والسطح الفاصل لخلايا بيروفسكايت المختلطة من هاليد الرصاص على كفاءتها واستقرارها. ركز العمل الحالي على تأثير كثافة العيوب ، ومساحة المقطع العرضي للعيوب ، ومستوى طاقة العيوب ، وأنواع العيوب في الطبقة الماصة على الكفاءة الكمية (QE) للخلية. علاوة على ذلك ، تم أيضًا دراسة تأثير العيوب في السطح الفاصل بين طبقة نقل الإلكترون / طبقة الامتصاص وطبقة نقل النقب / طبقة واجهات الامتصاص على نطاق واسع. في هذا العمل ، سيتم محاكاة الخلايا الشمسية الهجينة من الهاليد بيروفسكايت باستخدام محاكاة سعة الخلايا الشمسية أحادية البعد SCAPS-1D. يتكون هيكل الخلايا الشمسية من البيروفسكايت المقترح من FTO / ETM / ممتص / HTM على أساس TiO_2 كطبقة ETM ؛ Cu_2O كطبقة HTM ، وعلى $CH_3NH_3PbI_3$ كطبقة ماصة. وفقًا للنتائج ، انخفضت كفاءة الكم QE بشكل حاد من ٩٠.٢٪ إلى ٢٠٪ مع تغيير كثافة العيوب Nt ومساحة المقطع العرضي للعيوب σ في طبقة الامتصاص من 10^{10} سم^{-٣} إلى 10^{18} سم^{-٣} و 2×10^{-10} سم^٢ إلى 2×10^{-١٠} سم^٢ على التوالي. وجد أيضًا أن مساحة المقطع العرضي للالتقاط يُظهر سلوكًا مشابهًا لسلوك كثافة العيوب في الطبقة الماصة.

الكلمات المفتاحية: كفاءة الكم، خلايا بيروفسكايت الشمسية، العيوب، SCAPS-1D.



Study the effect of defects on the quantum efficiency of perovskite solar cells

Hajar Khalil Ibrahim Ahmed Mohammad Qais Thanon Algwari
Sabaawi

Ninevah University / College of Electronics Engineering/ Dept. of
Electronic

Abstract

Perovskite solar cells (PSCs) have generated considerable interest in the field of solar energy. With the rapid development of fabrication technology, high efficiency, environmentally friendly perovskite solar cells are becoming more attractive as candidates for power generation. Defects in the absorber and interface layers of mixed lead halide perovskite solar cells reduce the efficiency and stability of the cells. The current study examined the impact of defects density, defect capturing cross-section, defect level, and defect type on the quantum efficiency (QE) of the absorber layer. Furthermore, the impact of defects in the hole transport layer/absorber and electron transport layer/absorber interface layers is also be extensively studied. SCAPS-1D will be used to simulate perovskite solar cells in this work. The perovskite solar cells structure proposed is *FTO/ ETM/ absorber/ HTM* structure based on TiO_2 as *ETM* layer; Cu_2O as *HTM* layer, and on $CH_3NH_3PbI_3$ as absorber layer. According to the results, the quantum efficiency *QE* reduced sharply from 90.2% to 20% with varying the density of the defect *Nt* and the capture cross-section carriers σ in absorber layer from 10^{15} cm^{-3} to 10^{18} cm^{-3} and $2 \times 10^{-13} \text{ cm}^2$ to $2 \times 10^{-10} \text{ cm}^2$, respectively. Additionally, it is discovered that the capture cross-section carriers exhibits behavior similar to that of the absorber layer's defect density.

Keywords: quantum efficiency, perovskite solar cells, defects, SCAPS-1D.

1. Introduction

The latest generation of perovskite-based solar cells has experienced tremendous growth due to their affordability and ability to be easily processed [1]. Due to the high radiative efficiency of metal halide perovskites, *PSCs* exhibit a higher efficiency compared to a large variety of other types of solar cell, such as dye-sensitized solar cell, organic, and cadmium telluride solar cell. Given this impressive property, when perovskites are interfaced with inorganic materials such as gallium arsenide, they experience a higher non-radiative loss. This is caused by defects in the $CH_3NH_3PbI_3$ layer of perovskite. These defects demonstrate as three-dimension defect, such as precipitates, grain boundaries and dislocations, or as either point defect, such as anti-site substitutions, interstitials, and atomic vacancies. To free carriers from traps, the existence of a point defect inside the semiconductor band gap may create a recombination rate center, resulting in the formation of deep or shallow electron transformation levels in the banned region. This incident significantly decreases photoluminescence quantum efficiency (*QE*) and solar cells photovoltaic efficiency (*PCE*). The Shockley-Read-Hall recombination (*SRH*) can be described by:

$$R^{SRH} = \frac{v\sigma_n\sigma_p N_T (np - n_i^2)}{\sigma_p(p+p_1) + \sigma_n(n+n_1)} \quad (1)$$

where σ_n and σ_p are the electron capture cross-section area and hole capture cross-section area, v is the thermal velocity, N_T is the defects density, n_i is the intrinsic density, p and n are the hole and electron concentrations at balance, respectively, and n_1 and p_1 are the electron and hole concentrations in the defect of the trap and the valance band, respectively. R^{SRH} is proportional in a direct linear fashion to the defect density of the perovskite active layer [2]. The carriers diffusion duration is used to investigate the impact of defects concentration on the device's performance in terms of the SRH influence and the diffusion duration equation. According to Haider et al [3], As the defects densities of the perovskite active layer decreases, the diffusion length increases.

This phenomenon contributes to the improved performance of *PSCs*. The relations between carriers mobility, lifetime, and diffusion length is denoted by Equation 2 [4].

$$L_D = \sqrt{\frac{\mu_{(e,h)}KT}{q} \tau_{lifetime}} \quad (2)$$

The carriers mobility, diffusion length, and carrier lifetime are denoted by $\mu_{(e,h)}$, L_D , and $\tau_{lifetime}$, respectively. Equation (3) can be used to calculate the carriers diffusion length in the active layer, where D is the diffusion coefficient, which is defined as $D = \frac{\mu_{(e,h)}KT}{q}$ [5].

$$L_D = \sqrt{D \times \tau} \quad (3)$$

Equation 4 expresses the relationship between lifetime and bulk defect density. In the meantime, lifetime is dependent on the defect trap density and the area of the electron and hole capture cross-sections. The equation expresses the relationship between $\tau_{lifetime}$ and bulk defect density [4].

$$\tau_{lifetime} = \frac{1}{N_T \sigma v_{th}} \quad (4)$$

σ , v_{th} , and N_T denote, respectively, the capture cross-section of carriers, charge carriers' thermal velocity, and the defect density. Quantum efficiency (*QE*) is a critical characterization parameter for estimating a photovoltaic cell's performance. It is defined as the ratio of electron-hole pairs collected to photons impinging on the device. The *QE* value indicates the efficiency with which a photon is absorbed, an electron-hole pair is generated, separated, and then extracted via selective contacts [6]. The defect energy level is the location of the defect in the energy gap region. There have been insufficient studies conducted to date on the effect of defect mechanisms on quantum efficiency in *PSCs*. The purpose of this paper is to examine the effect of defects in a planer perovskite solar cell *PSC* structure composed of the following components: glass/*FTO*/*TiO₂*/*CH₃NH₃PbI₃*/*Cu₂O*/metal contact, which is designed to simulate using a 1-D Solar Cells Capacitance Simulator (*SCAPS-1D*) [7]. The present work investigates the effect of defect on quantum efficiency, with a particular emphasis on the defects

density, capture cross-section carriers in the $CH_3NH_3PbI_3$ active layers, and the defect density in the $CH_3NH_3PbI_3/HTM$ and $ETM/CH_3NH_3PbI_3$ interface layers. In addition, investigate the impact of defect level and defect types on quantum efficiency.

2. Device structure and parameters

SCAPS-1D was chosen for this study due to its widespread reputation as among the most efficient and user-friendly simulation software packages for modeling solar cells. As shown in Figure 1, a perovskite solar cell is a planar structure composed of FTO/TiO_2 (Electron Transportation Layer)/ $CH_3NH_3PbI_3$ (active layer)/ Cu_2O (Hole Transport Layer)/back contact. The values in Table 1 correspond to those found in the literature for the simulation parameters. The parameters of the defect in the active layer, the HTM /absorber, and the ETM /absorber interface layers of the PSC are summarized in Table 2.

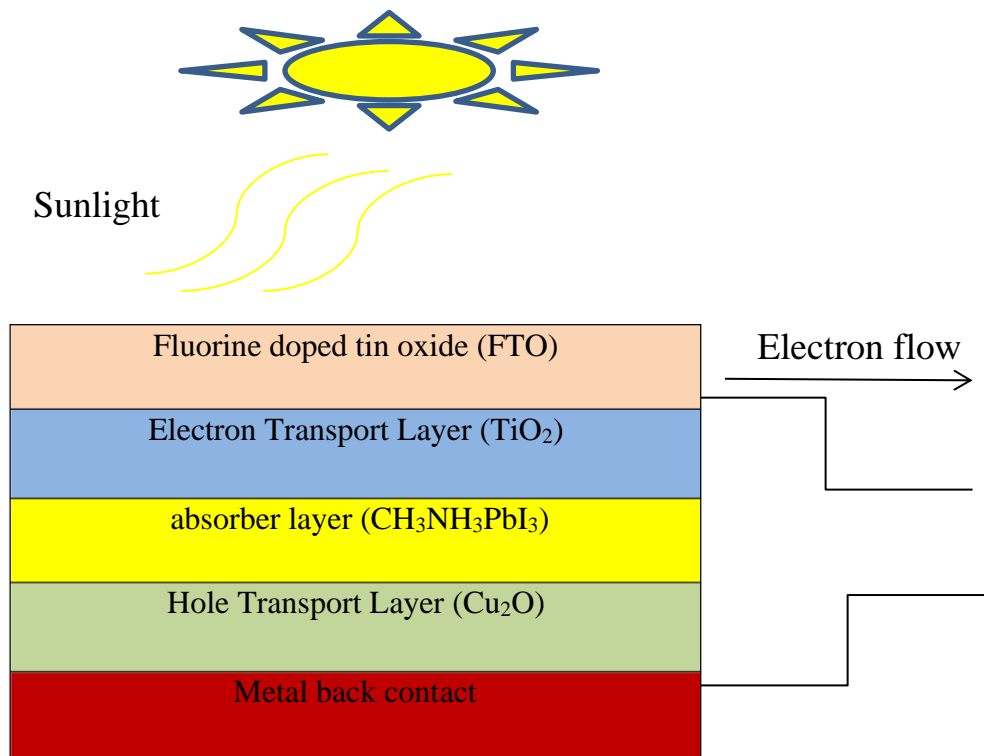


Fig. (1) The perovskite solar cell's basic structure.



Colleg

Parameter	FTO	TiO ₂	CH ₃ NH ₃ PbI ₃	Cu ₂ O
Thickness d (μm)	0.5	0.05	0.4	0.4
The band gap E _g (eV)	3.5	3.2	1.55	2.17
Electron affinity χ (eV)	4	3.9	3.9	3.2
Dielectric permittivity ϵ (relative)	9	9	6.5	6.6
CB effective density of state (1/cm ³)	2.2×10^{18}	1×10^{21}	2.2×10^{18}	2.5×10^{20}
VB effective density of state (1/cm ³)	1.8×10^{19}	2×10^{20}	1.8×10^{19}	2.5×10^{20}
Electron Mobility μ_n (cm ² /Vs)	20	20	2	80
Hole Mobility μ_p (cm ² /Vs)	10	10	2	80
Donor density N _D (1/cm ³)	2×10^{19}	1×10^{19}	0	0

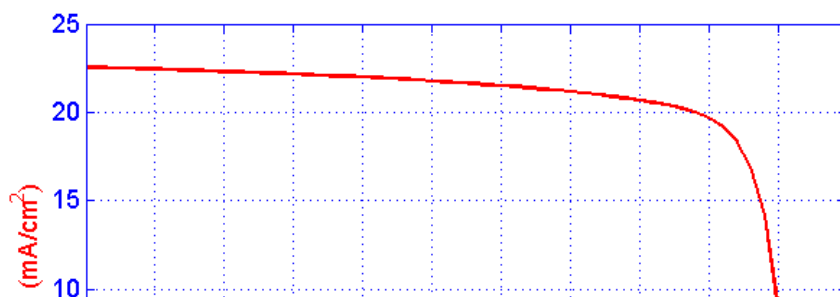
مجلة أبحاث كلية التربية الأساسية، المجلد ١٨، العدد (٢)، لسنة ٢٠٢٢
Table 1: Parameters for simulation of Perovskite solar cell devices [3], [8]–[12]
College of Basic Education Researchers Journal. ISSN: 7452-1992 Vol. (18), No.(2), (2022)

Acceptor density N_A ($1/\text{cm}^3$)	0	1	1×10^{15}	3×10^{18}
Electron thermal velocity v_{thn} (cm/s)	1×10^7	1×10^7	1×10^7	1×10^7
Hole thermal velocity v_{thp} (cm/s)	1×10^7	1×10^7	1×10^7	1×10^7

Table (1) Defect parameters of interface and absorber [3].

Parameter	Defect of absorber	Defect of HTM/Perovskite	Defect of ETM/Perovskite
Defect type	Neutral	Neutral	Neutral
Capture cross section electrons (cm^2)	2×10^{-15}	2×10^{-15}	2×10^{-16}
Capture cross-section holes (cm^2)	2×10^{-15}	2×10^{-15}	2×10^{-16}
Energetic distribution	Gaussian	Single	Single
Characteristic energy (eV)	0.1	0.1	0.1
Energy to reference (eV)	0.5	0.65	0.65
Total density ($1/\text{cm}^2$)	$(10^{10}-10^{18})$	1×10^{18}	1×10^{18}

Additionally, the defects density N_t in the $\text{CH}_3\text{NH}_3\text{PbI}_3$ layer is set to $2.5 \times 10^{13} \text{ cm}^{-3}$ using a Gaussian, while the defect density N_t in the another layers is set to 10^{15} cm^{-3} . The properties of absorber layer is that it is manufactured with specifications that make the values of defects in it differ from the rest of the layers, and this is what exists in practice. The defect energy level is set to the center of the bandgap energy with a characteristic energy level of 0.1 eV, the defect types is neutral, the electron and hole capturing cross-section is $2 \times 10^{-15} \text{ cm}^2$, a single distribution in the layers, and the absorber coefficient α is set to 10^5 cm^{-1} for each layer and $(1.5 \times 10^5) \text{ cm}^{-1}$ for the absorber layer [13]. The defect energy level in *ETM* and *HTM* layers are set to 0.6 eV. The spectrum of atmospheric conditions (air mass is AM1.5 G, temperature is 300 K) is used in the simulation. For operating point and numeric setting values, the default value is used. Between 0 and 1.3 V is used as the voltage range. The J-V current-voltage characteristics of a reference cell using Cu_2O as the *HTM* are illustrated in Figure (2), as well as the cell performance parameters for Cu_2O are: $PCE = 17.72\%$, $FF = 77.23\%$, $J_{sc} = 22.54 \text{ mA} \cdot \text{cm}^{-2}$, and $V_{oc} = 1.01 \text{ V}$.



3. Results and discussions

Defects reduce solar cell efficiency by introducing additional recombination processes (loss) and going to allow light to create heat instead of electricity. Defects in the semiconductor bandgap result in the formation of deep energy levels, reducing the carrier lifetime and quantum efficiency of solar cells.

3.1 The effect of defect density on quantum efficiency in the absorber layer

The influence of the defects density Nt in the $MAPbI_3$ layer on the quantum efficiency of perovskite solar cells was investigated by changing the defects density between 10^{10} cm^{-3} and 10^{18} cm^{-3} over a wavelength range of 300-800 nm. The defect level is set to 0.5 eV above the valance band [14], while all other parameters were kept constant such as capture cross-section in the absorber layer, which is set equals to $2 \times 10^{-15} \text{ cm}^2$, and total density in both HTM and ETM interfaces that are set to 10^{18} cm^{-2} . The results are presented in Figure (3).

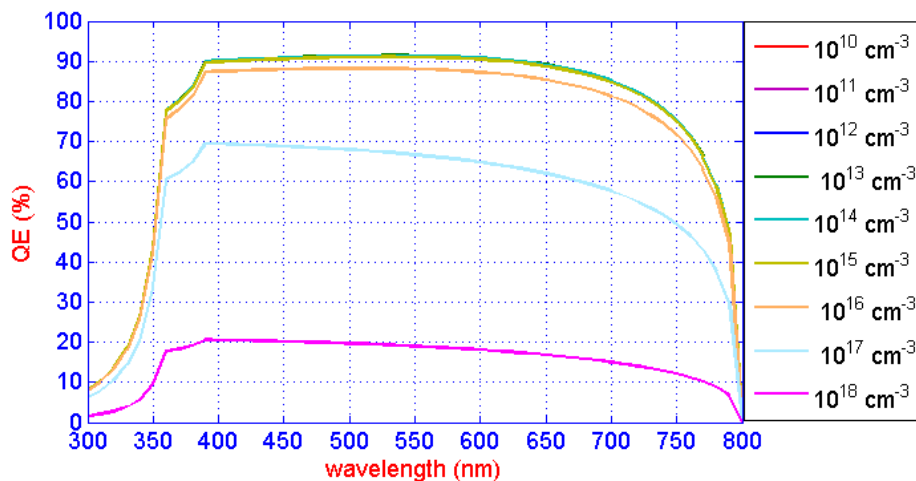
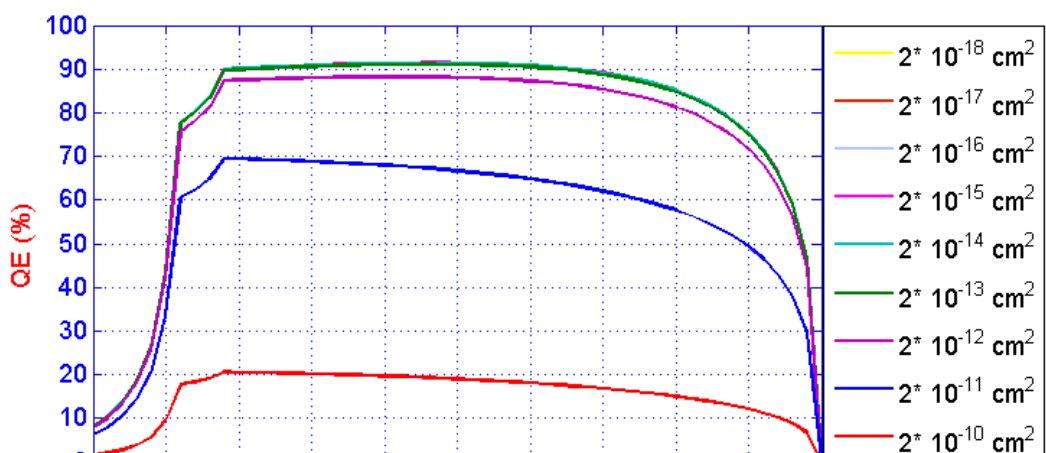


Fig. (3) Quantum efficiency of PSC with a variation of defect density in the

It can be shown in Figure (3) that the maximum achieved quantum efficiency is about 90.2% within the wavelength range from 390 nm to 650 nm for defect densities from 10^{10} cm^{-3} to 10^{15} cm^{-3} . Furthermore, the *QE* declines sharply for defect densities higher than 10^{15} cm^{-3} to reach only 20% at an exponential rate. This indicates that the defect density *Nt* in the *MAPbI₃* active layer of 10^{15} cm^{-3} or lower is able to absorb the majority of incident photons, and the rest does not make a significant contribution to the cell since the defect density affects the recombination of the photogenerated electron-hole pairs in the active layer.

3.2 The effect of capture cross-section on quantum efficiency in the absorber layer

The influence of capturing cross-section σ in *MAPbI₃* layer on the quantum efficiency of *PSCs* has been studied by varying the capturing cross-section area of carriers from $2 \times 10^{10} \text{ cm}^2$ to $2 \times 10^{-18} \text{ cm}^2$ and computing the *QE* over a wavelengths range from 300 nm to 800 nm as illustrated in Figure (4). The defect level was set to 0.5 eV above the valance band [14], while all other parameters were kept constant. The energy level of defects in the absorbing layer was chosen near to the valance band due to any small energy absorbed by the electron from the incident light helps to stimulate the electron to the defect energy level and thus this electron is lost from the overall transition process.



As it is seen in Figure (4), the maximum quantum efficiency QE achieved is approximately 90.2 % within the wavelength range of 390 nm to 650 nm for capture cross-section area σ varies from $2 \times 10^{-18} \text{ cm}^2$ to $2 \times 10^{-13} \text{ cm}^2$. Additionally, the QE decreases rapidly for capture cross-section greater than $2 \times 10^{-13} \text{ cm}^2$, eventually reaching only 20% at an exponential rate. The capture cross section of the $MAPbI_3$ layer is sufficient to improve the performance of PSC cells. The quantum efficiency depends on the number of charge carriers, and since the thickness of the $MAPbI_3$ absorber layer is relatively large compared to the thickness of the interface layer, the charge carriers will take a longer time to complete their path to pass this layer and therefore the possibility of capturing it increases and therefore defects in the $MAPbI_3$ layer reduce the charge carriers, which is reflected on the efficiency. The probability of trapping increases with the increase in the cross-section.

3.3 The effect of defect level on quantum efficiency in the absorber layer

The influence of defect level in $MAPbI_3$ active layer on the quantum efficiency of $PSCs$ perovskite solar cells has been evaluated, where the defects level was varied from 0.2 eV to 1.2 eV and over a wavelengths range from 300 nm to 800 nm. The quantum efficiency has a maximum value of about 90.2% and it is obtained through the program SCAPS. The result demonstrated that the quantum efficiency has shown no change with increasing the defect level. This indicates that choosing any energy level in the $MAPbI_3$ absorber layer has no noticeable effect on the performance of $PSCs$. Due to the transfer

of electrons through the light absorption process will cross the energy band, so the probability that the electron will be captured during the transition process is constant with all the defect levels in the energy gap region.

3.4 The effect of defect types on quantum efficiency in the absorber layer

The influence of defect types in $MAPbI_3$ layer on the quantum efficiency of PSC has been investigated where various defect types (neutral, single acceptor, single donor double donor, double acceptor, and amphoteric) are selected over a wavelengths range from 300 nm to 800 nm as shown in

Table 3. Variation of defect type in absorber layer on quantum efficiency

Defect type	Quantum efficiency $QE\%$
Neutral	91.30
Single donor	91.29
Single acceptor	91.31
Double donor	91.30
Double	91.35
Amphoteric	91.33

From

, it can be seen that the quantum efficiency is unaffected by the defect type and almost remains unchanged at about 91%. As a result, it is found that the defect type does not affect the quantum efficiency of the $PSCs$. To explain this phenomenon, the properties of defects are defects density and capture cross-sectional. These properties are common to all defects, and therefore the type no affect on QE .

3.5 The effect of defect density on quantum efficiency in HTM interface layer

The influence of defects density Nt in the $HTM/MAPbI_3$ interface layer on the quantum efficiency of PSC has been extensively studied by changing the defect density Nt from 10^{11} cm^{-3} to 10^{20} cm^{-3} at a wavelength of 500 nm as a reference. The defect level was set to 0.5 eV above the valance band. The results are shown in .

Table 4. Quantum efficiency with a varying defect density of PSC in *HTM*/absorber interface layer.

defect density Nt (cm^{-3})	Quantum efficiency QE %
1×10^{11}	91.82
1×10^{12}	91.65
1×10^{13}	91.36
1×10^{14}	91.31
1×10^{15}	91.30
1×10^{16}	91.30
1×10^{17}	91.30
1×10^{18}	91.30
1×10^{19}	91.30
1×10^{20}	91.30

It is observed from that the quantum efficiency is almost remained constant at about 91% when the Nt was increased within the range of the test. This shows that increasing the defect density Nt in *HTM/MAPbI₃* interface layer had no obvious impact on quantum efficiency. The interfaces *HTM/MAPbI₃* and the *MAPbI₃/ETM* do not take part in the photoelectric effect directly as they are wide-gap materials that will pass the solar radiation without absorbing it.

3.6 The effect of defect density on quantum efficiency in *ETM* interface layer

To investigate the impact of differing the defects density of the *TiO₂/MAPbI₃* interface layer on a solar cell's quantum efficiency, the defect density Nt was varied between $10^{11} cm^{-3}$ and $10^{20} cm^{-3}$ while maintaining all other parameters constant. All results were recorded at 500 nm wavelength as a reference, as shown in Table 5.

Table 5. Quantum efficiency variation with the defects density in the ETM interface layer.

Defect density Nt (cm^{-3})	Quantum efficiency QE %
1×10^{11}	98.90
1×10^{12}	98.72
1×10^{13}	97.32
1×10^{14}	93.39
1×10^{15}	91.58
1×10^{16}	91.33
1×10^{17}	91.30
1×10^{18}	91.30
1×10^{19}	91.30
1×10^{20}	91.30

It is found that the quantum efficiency decreases from 98.9 % to 91.5 % when the defect density Nt is less than 10^{15} cm^{-3} ; however, when the defect density Nt is greater than 10^{15} cm^{-3} , the quantum efficiency remains constant at around 91.3 %. Additionally, the defects density in the *ETM* interface layer has a negligible impact on the quantum efficiency of *PSCs*.

3.7 The effect of capture cross-section on quantum efficiency in *HTM* and *ETM* interface layers

The impact of capturing cross-section for electron σ_n and hole σ_p in *HTM/MAPbI₃* and *MAPbI₃/ETM* on quantum efficiency has been extensively studied. The capture cross-section-carriers σ is varied from $2 \times 10^{-10} \text{ cm}^3$ to $2 \times 10^{-18} \text{ cm}^3$ at a wavelength of 500 nm as a reference, while other parameters are kept unchanged, such as the defects density in the active layer, which is set to $2.5 \times 10^{13} \text{ cm}^{-3}$ and total density in both *HTM* and *ETM* interfaces that set to 10^{18} cm^{-3} . The defect level was set to 0.5 eV above the valance band. It is observed that the quantum efficiency was unchanged (91.3 %) with increasing

the capture cross-section, and it is obtained through the program SCAPS. Which indicates that the quantum efficiency of perovskite solar cells had shown no obvious change with varying the capture cross-section area in both interface layers. The quantum efficiency depends on the number of charge carriers, and since the thickness of the separating layer is small compared to the thickness of the absorber layer, the charge carriers spend a relatively short time when passing through it, so the possibility of capture is less.

3.8 The impact of defect level on the quantum efficiency at interfaces layer

The effect of increasing the defect level in the $MAPbI_3/Cu_2O$ and $TiO_2/MAPbI_3$ interface layers on the quantum efficiency of PSC has been investigated; the quantum efficiency varies as the defect level is increased from 0.2 eV to 1.2 eV while maintaining other parameters constant at a reference wavelength of 500 nm. As can be seen, the quantum efficiency QE remained constant at approximately 91 % as the defect level in the interface layers increased. This indicates that varying the defect level in the *HTM* and *ETM* interface layers has no effect on the quantum efficiency of perovskite solar cells. Due to the fact that electrons will cross the energy band during the light absorption process, the probability of an electron being captured during the transition process is constant for all defect levels in the energy gap region.

4. Conclusions

In the present work, the impact of different defects parameters such as defects density Nt , capturing cross-section σ , defect type, and defect energy level in absorber layer, *HTM*/absorber and *ETM*/absorber interface layers on the quantum efficiency QE were studied. Planer structure $FTO/TiO_2/CH_3NH_3PbI_3/Cu_2O$ were investigated using a 1-D Solar Cells Capacitance Simulator (SCAPS-1D). In an absorber layer, the quantum efficiency was reduced sharply from 90.2% to 20% at defect density and capture cross-section varies from 10^{15} cm^{-3} to 10^{18} cm^{-3} and from $2 \times 10^{-13} \text{ cm}^2$ to $2 \times 10^{-10} \text{ cm}^2$, respectively. Additionally, it was noticed that the defects density in *HTM* interface layer and capturing cross-section area of carrier in *ETM* and *HTM* interface layers had no impact on quantum efficiency. In addition, it was observed that the quantum efficiency of perovskite solar cells suffers a slight reduction with increasing defect density in *ETM/MAPbI_3* interface. Defect energy level has also no significant impact on the PSC performance neither in the $MAPbI_3$ absorber layer nor in the *HTM*/absorber and absorber/*ETM* interfaces layers.

Thanks and appreciation

The authors would like to thank the collage of Electronics Engineering and the Electronic Engineering department at Ninevah University for their support.

References

- [1] Shubham, Raghvendra, C. Pathak, and S. K. Pandey, "Design, Performance, and Defect Density Analysis of Efficient Eco-Friendly Perovskite Solar Cell," *IEEE Trans. Electron Devices*, vol. 67, no. 7, pp. 2837–2843, 2020, doi: 10.1109/TED.2020.2996570.
- [2] S. Mahjabin *et al.*, "Perceiving of Defect Tolerance in Perovskite Absorber Layer for Efficient Perovskite Solar Cell," *IEEE Access*, vol. 8. pp. 106346–106353, 2020, doi: 10.1109/ACCESS.2020.3000217.
- [3] S. Z. Haider, H. Anwar, and M. Wang, "A comprehensive device modelling of perovskite solar cell with inorganic copper iodide as hole transport material," *Semicond. Sci. Technol.*, vol. 33, no. 3, p. 35001, 2018.
- [4] M. S. Jamal *et al.*, "Effect of defect density and energy level mismatch on the performance of perovskite solar cells by numerical simulation," *Optik (Stuttg.)*, vol. 182, pp. 1204–1210, 2019.
- [5] S. Abdelaziz, A. Zekry, A. Shaker, and M. Abouelatta, "Investigating the performance of formamidinium tin-based perovskite solar cell by SCAPS device simulation," *Opt. Mater. (Amst.)*, vol. 101, no. January, p. 109738, 2020, doi: 10.1016/j.optmat.2020.109738.
- [6] S. Ravishankar, C. Aranda, P. P. Boix, J. A. Anta, J. Bisquert, and G. Garcia-Belmonte, "Effects of Frequency Dependence of the External Quantum Efficiency of Perovskite Solar Cells," *J. Phys. Chem. Lett.*, vol. 9, no. 11, pp. 3099–3104, 2018, doi: 10.1021/acs.jpcllett.8b01245.
- [7] K. Tan, P. Lin, G. Wang, Y. Liu, Z. Xu, and Y. Lin, "Controllable design of solid-state perovskite solar cells by SCAPS device simulation," *Solid. State. Electron.*, vol. 126, pp. 75–80, 2016.
- [8] F. Azri, A. Meftah, N. Sengouga, and A. Meftah, "Electron and hole transport layers optimization by numerical simulation of a perovskite solar cell," *Sol. energy*, vol. 181, pp. 372–378, 2019.



- [9] L. Lin, L. Jiang, Y. Qiu, and Y. Yu, "Modeling and analysis of HTM-free perovskite solar cells based on ZnO electron transport layer," *Superlattices Microstruct.*, vol. 104, pp. 167–177, 2017.
- [10] K. Sobayel *et al.*, "A comprehensive defect study of tungsten disulfide (WS₂) as electron transport layer in perovskite solar cells by numerical simulation," *Results in Physics*, vol. 12, pp. 1097–1103, 2019, doi: 10.1016/j.rinp.2018.12.049.
- [11] A. S. Chouhan, N. P. Jasti, and S. Avasthi, "Effect of interface defect density on performance of perovskite solar cell: Correlation of simulation and experiment," *Mater. Lett.*, vol. 221, pp. 150–153, 2018, doi: 10.1016/j.matlet.2018.03.095.
- [12] G. A. Casas, M. A. Cappelletti, A. P. Cedola, B. M. Soucase, and E. L. P. y Blancá, "Analysis of the power conversion efficiency of perovskite solar cells with different materials as Hole-Transport Layer by numerical simulations," *Superlattices Microstruct.*, vol. 107, pp. 136–143, 2017.
- [13] Y. Li *et al.*, "Direct Observation of Long Electron-Hole Diffusion Distance in CH₃NH₃PbI₃ Perovskite Thin Film," *Sci. Rep.*, vol. 5, no. April, pp. 1–8, 2015, doi: 10.1038/srep14485.
- [14] S. Huang, Z. Rui, D. Chi, and D. Bao, "Influence of defect states on the performances of planar tin halide perovskite solar cells," *J. Semicond.*, vol. 40, no. 3, 2019, doi: 10.1088/1674-4926/40/3/032201.